# **Green Chemistry**



PAPER View Article Online View Journal



Cite this: DOI: 10.1039/c7gc01188a

# Selective conversion of bio-derived ethanol to renewable BTX over Ga-ZSM-5†

Zhenglong Li,<sup>a</sup> Andrew W. Lepore,<sup>b,c</sup> Mariam F. Salazar,‡<sup>b</sup> Guo Shiou Foo,<sup>d</sup> Brian H. Davison, <sup>©</sup> <sup>e</sup> Zili Wu<sup>d,f</sup> and Chaitanya K. Narula <sup>©</sup> \*<sup>b,c</sup>

Selective conversion of bio-derived ethanol to benzene, toluene and xylenes (BTX) is desirable for producing renewable BTX. In this work, we show that addition of Ga to H-ZSM-5 leads to a two-fold increase in the BTX yield as compared with H-ZSM-5 when ethanol is converted over these zeolites at 450 °C and ambient pressure. Besides promoting BTX formation, Ga also plays an important role in enhancing molecular hydrogen production and suppressing hydrogen transfer reactions for light alkane formation. The ion exchange synthesis of Ga-ZSM-5 results in the majority of Ga at the outer surface of zeolite crystals as extra-zeolitic Ga<sub>2</sub>O<sub>3</sub> particles and only a small fraction of Ga exchanging with the Brønsted acid sites which appears to be responsible for higher ethanol conversion to BTX. The interface between H-ZSM-5 and Ga<sub>2</sub>O<sub>3</sub> particles is not active since H-ZSM-5 and the physical mixture of β-Ga<sub>2</sub>O<sub>3</sub>/H-ZSM-5 furnish an almost identical product distribution. Hydrogen reduction of the physical mixtures facilitates movement of Ga to ion exchange locations and dramatically increases the BTX yield becoming comparable to those obtained over ion-exchanged Ga-ZSM-5, suggesting that exchanged Ga(III) cations are responsible for the increased BTX production. A linear correlation between the BTX site time yield and exchanged Ga sites further confirms that Ga occupying cationic sites are active sites for enhancing BTX formation. Reduction of physical mixtures ( $\beta$ -Ga<sub>2</sub>O<sub>3</sub>/H-ZSM-5) also provides an economical and environmentally friendly non-aqueous method for large scale catalyst synthesis without sacrificing catalyst performance for ethanol conversion application.

Received 19th April 2017, Accepted 19th May 2017 DOI: 10.1039/c7gc01188a

rsc.li/greenchem

# 1. Introduction

Ethanol derived from a biomass fermentation process is one of the most successful biofuels in the commercial market with a 90% share of global biofuel production. Driven by the innovative cellulosic ethanol technology, global ethanol production is increasing rapidly and anticipated to reach more than 33 billion gallons in 2017. The ethanol market is at a sat-

In recent years, the conversion of ethanol to various chemicals and fuels, e.g., ethylene, 6,7 C3-C4 olefins, butanol, 9-11 butadiene, 12-14 and gasoline 15 has been reported. Benzene, toluene and xylenes (BTX), mainly produced from petroleum, are valuable commodity chemicals and are among the most abundantly produced chemicals with worldwide annual production of 9-11 million tons of benzene, 13-14 million tons of toluene and 17 million tons of xylenes.16 However, there are limited reports on BTX production from bio-derived ethanol.<sup>1</sup> The focus has been on optimizing H-ZSM-5 to improve the BTX yield, including varying the Si/Al ratios and introducing metal promoters. 17 Barthos et al. have shown that modified ZSM-5 with Mo<sub>2</sub>C and ZnO promoted the formation of benzene and toluene at 500-700 °C.18,19 A catalyst containing Ga has also been reported for ethanol conversion<sup>20,21</sup> as Ga is a very important promoter for upgrading light alkanes.<sup>22-24</sup> For example, Saha and Sivasanker report that ethanol conversion over Ga-ZSM-5 at 360 °C and 10 atm results in improved

uration point in the US transportation sector since its use is limited by the 10–15% blend-wall due to technological and infrastructure constraints.<sup>5</sup> The excess ethanol will be available as a platform molecule for the production of liquid hydrocarbon fuels and value-added chemicals in the future.

<sup>&</sup>lt;sup>a</sup>Energy & Transportation Sciences Division, Oak Ridge National Laboratory, Oak Ridge, TN 37831, USA

<sup>&</sup>lt;sup>b</sup>Materials Science & Technology Division, Oak Ridge National Laboratory, Oak Ridge, TN 37831, USA

<sup>&</sup>lt;sup>c</sup>Bredesen Center for Interdisciplinary Research, 821 Volunteer Blvd., The University of Tennessee, Knoxville, TN 37996, USA. E-mail: narulack@ornl.gov

<sup>&</sup>lt;sup>d</sup>Chemical Sciences Division, Oak Ridge National Laboratory, Oak Ridge, TN 37831, USA

<sup>&</sup>lt;sup>e</sup>BioSciences Division, Oak Ridge National Laboratory, Oak Ridge, TN 37831, USA <sup>f</sup>The Center for Nanophase Materials Sciences, Oak Ridge National Laboratory, Oak Ridge, TN 37831, USA

<sup>†</sup>Electronic supplementary information (ESI) available. See DOI: 10.1039/c7gc01188a

<sup>‡</sup>Current address: Technip Stone & Webster Process Technology, Inc., 56 Woodrock Rd, Weymouth, MA 02189, USA.

Published on 01 June 2017. Downloaded by University of Tennessee at Knoxville on 01/09/2017 21:30:59

**Paper** 

temperature under a flow of 45 ml min<sup>-1</sup> helium and 5 ml min<sup>-1</sup> nitrogen.

catalyst stability.  $^{20}$  However, Ga-ZSM-5 only shows a 4% increase of the BTX yield as compared to that over H-ZSM-5. Borght *et al.* found that <1.0 wt% Ga loading on H-ZSM-5 has a minor positive effect on the  $\rm C_{5+}$  hydrocarbon production from ethanol conversion at 350 °C and ambient pressure.  $^{21}$  None of these studies clearly show the dramatic Ga promotion of BTX compared with H-ZSM-5. More importantly, there is practically no information on the role and the nature of the active Ga species for ethanol conversion.

Here, we clearly demonstrate that the addition of Ga to H-ZSM-5 leads to a two-fold increase in the BTX yield and report optimum Ga loading and reaction temperatures (at and above 450 °C). We also present our studies on catalyst characterization and testing to infer the role of active Ga species. The effects of temperature, space velocity and Ga loading on the catalyst activity and product distributions are discussed. These results clearly show that Ga promotes BTX formation and hydrogen production and suppresses hydrogen transfer reactions. Our results on acid site measurements and catalytic activity of Ga-ZSM-5 and Ga<sub>2</sub>O<sub>3</sub>/H-ZSM-5 physical mixtures enable us to correlate catalyst activity with the proposed active Ga species. The hydrogen treatment of a physical mixture is a convenient, economical, and environmentally friendly non-aqueous method for large scale Ga-ZSM-5 catalyst synthesis for ethanol conversion.

# 2. Experimental

#### 2.1 Catalyst synthesis

Commercial NH<sub>4</sub>-ZSM-5 (CBV2314) was purchased from Zeolyst Corporation and used as received. Ga-ZSM-5 was prepared by an ion exchange method.  $NH_4$ -ZSM-5 (SiO<sub>2</sub>/Al<sub>2</sub>O<sub>3</sub> = 23) (2.4 g) was suspended in a solution of a known amount of Ga(NO3)3 in 120 mL of distilled water. The reaction mixture was heated to 80 °C with stirring, kept at that temperature for 16 h, and centrifuged to separate the solids. The recovered solid was washed twice with 120 ml DI water and dried at 105 °C overnight. Subsequently, the solids were calcined at 500 °C for 6 h. Ga loadings were controlled by varying the  $Ga(NO_3)_3$  solution concentrations or exchanging time. Physical mixtures of H-ZSM-5 and β-Ga<sub>2</sub>O<sub>3</sub> with different Ga loadings were prepared by mixing known amounts of H-ZSM-5 and β-Ga<sub>2</sub>O<sub>3</sub>, grinding for 30 min, pelletizing, and grinding to the size of 125-250 μm. This was done to ensure intimate contact between H-ZSM-5 and β-Ga<sub>2</sub>O<sub>3</sub>. The physical mixture reduction pretreatment was performed under a 40 ml min<sup>-1</sup> (standard conditions unless otherwise stated) hydrogen flow at 500 °C for 2 h.

#### 2.2 Catalytic conversion of ethanol

A quartz reactor (8 mm ID  $\times$  25 cm H) was loaded with 0.2 g of catalyst (125–250 µm) between two layers of quartz wool. Two thermocouples were used to measure the gas inlet and catalyst bed temperatures. All the reported temperatures in this paper are catalyst bed temperatures unless otherwise stated. A tube furnace was used to heat the catalyst up to the desired reaction

Pure ethanol was fed into the reactor at a rate of 0.4 ml h<sup>-1</sup> employing a syringe pump which translates into a weight hourly space velocity (WHSV, g ethanol per g catalyst h) of 1.6 h<sup>-1</sup>. For the physical mixture experiments, the ethanol space velocity is based on the mass of H-ZSM-5 in the mixture. After running the reaction for 2 h, the ethanol flow was stopped and the physical mixtures were reduced under hydrogen at 500 °C for 2 h and then ethanol was restarted after cooling down to 450 °C. For space velocity study, the ethanol flow rate and total gas flow varied proportionally to meet the desired space velocity while maintaining ethanol partial pressure in the feed stream. The reactions were run for 1.0 h prior to product analysis with an on-line gas chromatograph (Agilent 7820A) employing a HP-Plot Q capillary column (dimension of 30.0 m  $\times$  320  $\mu$ m  $\times$  20.0  $\mu$ m) and a FID detector. The transfer line between the reactor and the GC/FID was heated to ~250 °C to prevent condensation of heavy products. For analysis, GC was held at 50 °C for 3 min, ramped up to 250 °C at a rate of 15 °C min<sup>-1</sup> and then held at that temperature for 35 min. A constant pressure mode of 9.51 psi was used and the inlet temperature was 250 °C. A gas calibration mixture (6% ethylene, 3% propene, 3% propane, 2% cis-2butene, 1.04% isobutene, 1000 ppm isobutane and balance nitrogen) was used to calibrate C2 to C4 hydrocarbons. Standards of benzene, toluene, p-xylene, ethylbenzene and cumene were used to quantify aromatic compounds. All of the reported product yields are wt% unless otherwise stated.

#### 2.3 Catalyst characterization

Elemental analyses were performed using inductively coupled plasma (ICP) by Galbraith Incorporated, Knoxville, TN, United States. All the reported metal loadings are based on weight except otherwise stated. Powder X-ray diffraction (XRD) data were obtained on the Panalytical X'pert diffractometer from 5 to 80°  $2\theta$  in 30 min scans using Cu K $\alpha$  radiation (45 kV, 40 mA,  $\lambda$  = 1.5406 Å). The lattice parameters for the ZSM-5 phase are obtained through Rietveld refinements.

The chemical compositions and oxidation states of the surface species were analyzed by X-ray photoelectron spectroscopy (XPS) using a Thermo Scientific K-Alpha XPS instrument. The K-Alpha uses Al–K $\alpha$  X-rays focused to a spot 400  $\mu$ m in diameter. Emitted photoelectrons were analyzed using a 180° double focusing hemispherical analyzer with a 128-channel detector. Survey data were collected at a pass energy of 200 eV and an energy resolution of 1 eV per step, while core level data were collected at 50 eV pass energy and 0.1 eV per step energy resolution. Sample charging was eliminated by using the K-Alpha's dual-beam charge compensation source which uses both low energy Ar-ions and low energy electrons. Data were collected and analyzed using the Avantage data system (v.4.61).

*n*-Propylamine temperature-programmed desorption (TPD) experiments were performed using an Altamira Instruments System (AMI-200). Each sample (~10 mg) was loaded into a

**Green Chemistry** Paper

quartz U-tube and the catalyst bed was held in place by quartz wool at both ends. The samples were heated to 550 °C at a ramp rate of 5 °C min<sup>-1</sup> under He for 1 h. The samples were then cooled down to 50 °C and saturated by flowing 30 ml min<sup>-1</sup> of 1000 ppm *n*-propylamine (balance argon, Airgas) for 2 h. Subsequently, the samples were purged with 30 ml min<sup>-1</sup> of argon (Airgas) for 6 h. The temperature was increased to 600 °C at a ramp rate of 10 °C min<sup>-1</sup> and held for 1 h. During this period, the reactor effluent was monitored by using a Pfeiffer Vacuum OmniStar GSD 301 O2 mass spectrometer. All of the lines were heated to 100 °C. After each TPD experiment, the mass spectrometer was calibrated by pulsing various concentrations of propene mixed with argon through a 507 µL sample loop.

NH<sub>3</sub> temperature-programmed desorption (TPD) experiments were performed in a U-tube reactor with an Eco Physics NOx analyzer. The NOx analyzer was calibrated each time before use using 100 ml min<sup>-1</sup> 2500 ppm ammonia balanced in argon. Each sample (~50 mg) was loaded into a quartz U-tube reactor. The samples were pretreated under 50 ml min<sup>-1</sup> Ar flow at 550 °C for 1 h at a ramp rate of 5 °C min<sup>-1</sup>. The samples were cooled down to 120 °C and saturated by flowing 100 ml min<sup>-1</sup> of 2500 ppm ammonia (balance argon) for 1 h. Subsequently, the samples were purged with 100 ml min<sup>-1</sup> of argon for 1.5 h. The temperature was increased to 600 °C at a ramp rate of 10 °C min<sup>-1</sup> and held for 1 h for the temperature-programmed desorption.

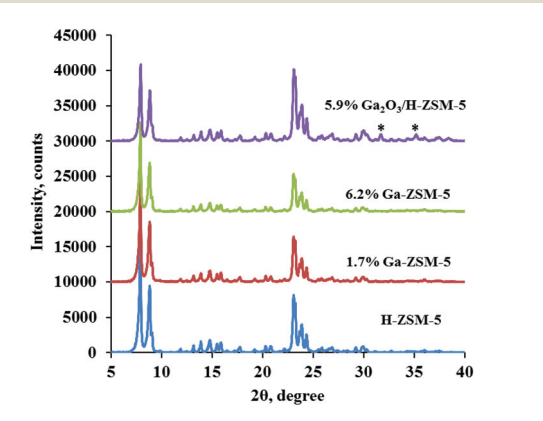


Fig. 1 X-ray diffraction patterns for H-ZSM-5, 1.7% Ga-ZSM-5, 6.2% Ga-ZSM-5 and physical mixture of 5.9% Ga<sub>2</sub>O<sub>3</sub>/H-ZSM-5, \* indicates peaks for Ga<sub>2</sub>O<sub>3</sub>.

#### Results & discussion 3.

#### Catalyst characterization

All Ga-ZSM-5 catalysts (Ga loading up to 6.2%), prepared by an ion exchange method (described as x% Ga-ZSM-5 where x is Ga loading), show identical X-ray diffraction patterns to H-ZSM-5 (Fig. 1), suggesting that the zeolite structure remains unchanged after Ga loading. There are also no unit cell size changes after the addition of Ga with all unit cell sizes falling in the range of 5378 to 5392 Å<sup>3</sup> (Table S1†). The physical mixture of 5.9% Ga<sub>2</sub>O<sub>3</sub>/H-ZSM-5 (described as x% Ga<sub>2</sub>O<sub>3</sub>/ H-ZSM-5 where x% is  $Ga_2O_3$  loading) shows the  $Ga_2O_3$  phase, while none of the Ga-ZSM-5 show Ga<sub>2</sub>O<sub>3</sub> peaks. The absence of Ga<sub>2</sub>O<sub>3</sub> peaks from XRD analysis could be due to the presence of exchanged Ga cations, amorphous oxide, or small particles.

The total acidity and the Brønsted acidity of H-ZSM-5 and Ga-ZSM-5 catalysts are shown in Table 1. The number of Brønsted acid sites decreases with increase in Ga loading while only slight changes are observed in the number of total acid sites. Gallium exchange with the Brønsted acid sites is very likely to be the reason for the decrease in the Brønsted acid sites. Only a small fraction of Ga is present as exchanged Ga cations for Ga-ZSM-5 with Ga loadings from 0.5% to 6.2% (Table 1). The remaining Ga exists as extra-zeolitic Ga<sub>2</sub>O<sub>3</sub>. This observation is consistent with a previous report from Nowak et al. who observed that Ga is mainly present as Ga2O3 particles at the outer surface of zeolite crystals via high-resolution TEM for Ga-ZSM-5 after calcination at 550 °C. 25 This is because Ga is predominantly present in the hydrated form and isolated Ga<sup>3+</sup> comprise only a small fraction in aqueous solution during the ion exchange process.26 The hydrated Ga3+ species cannot enter the elliptical  $(0.55 \times 0.57 \text{ nm})$  channels during ion exchange resulting in gallium deposition as extrazeolitic oxide on the outer surface of zeolite crystals. 26 Our XPS analysis (Table S2†) also suggests that the major fraction of Ga is on the external surface of zeolite.

#### 3.2 Conversion of ethanol over Ga-ZSM-5

3.2.1 Impact of temperature. Ethanol conversion over Ga-ZSM-5 is complete in the temperature range of 300-500 °C (Fig. 2) at a WHSV of 1.6  $h^{-1}$ . The liquid (C<sub>5+</sub>) hydrocarbon yield increases with increase in temperature to 450 °C and reaches a plateau (46%) above this temperature. The liquid hydrocarbon composition shifts toward BTX formation above 350 °C as indicated by the increased BTX fraction in C5+

Table 1 The total acidity, Brønsted acidity and exchanged Ga for Ga-ZSM-5 with different Ga loadings

|               | Ga loading (wt%) | Total acids <sup>a</sup> (µmol g <sup>-1</sup> ) | Brønsted acids $^b$ ( $\mu$ mol $g^{-1}$ ) | Exchanged Ga <sup>c</sup> (µmol g <sup>-1</sup> ) | Exchanged Ga <sup>d</sup> (%) |
|---------------|------------------|--|--|---|-------------------------------|
| H-ZSM-5       | 0.0              | 1029   | 730  | 0   | 0                             |
| 0.5% Ga-ZSM-5 | 0.5              | 1030   | 720  | 5.1   | 7.2                           |
| 1.7% Ga-ZSM-5 | 1.7              | 932  | 683  | 30  | 13                            |
| 6.2% Ga-ZSM-5 | 6.2              | 991  | 548  | 122   | 14                            |

 $<sup>^</sup>a$  The total acidity is measured by NH<sub>3</sub>-TPD.  $^b$  The Brønsted acidity is measured by n-propylamine TPD.  $^c$  The amount of exchanged Ga is calculated based on the Brønsted acidity decrease relative to H-ZSM-5.  $^{22}$   $^d$  The percentage of exchanged Ga among the total Ga.

**Paper** 

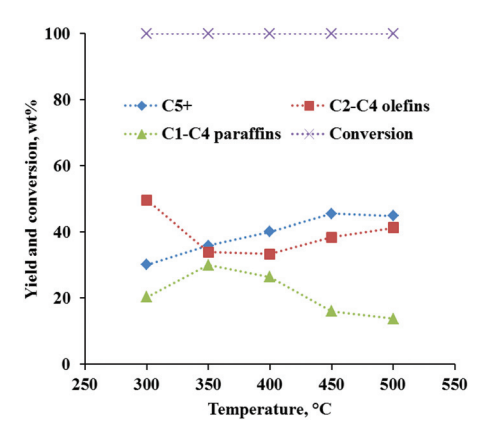


Fig. 2 Ethanol conversion and product yields over 1.7% Ga-ZSM-5 at  $1.6\ h^{-1}$ .

**Table 2**  $C_1$ – $C_4$  product distributions, and BTX and  $C_{5+}$  yields for ethanol conversion over 1.7% Ga–ZSM-5 at 1.6 h<sup>-1</sup>

|                                      | Temperature, °C |      |      |      |      |  |
|--------------------------------------|-----------------|------|------|------|------|--|
| Products                             | 300             | 350  | 400  | 450  | 500  |  |
| CH <sub>4</sub>                      | 0.1             | 0.5  | 2.0  | 3.6  | 4.3  |  |
| $C_2H_4$                             | 36.3            | 20.3 | 21   | 31   | 34   |  |
| $C_2H_6$                             | 0.6             | 1.6  | 2.8  | 3.2  | 3.6  |  |
| $C_3H_6$                             | 6.9             | 8.4  | 8.6  | 6.2  | 5.9  |  |
| $C_3H_8$                             | 4.0             | 8.0  | 8.0  | 5.6  | 4.7  |  |
| Isobutane                            | 11.9            | 15.7 | 10.4 | 2.0  | 0.5  |  |
| 2-Butene                             | 5.2             | 4.3  | 2.7  | 1.0  | 0.8  |  |
| Butane                               | 3.9             | 4.3  | 3.4  | 0.6  | 0.9  |  |
| Isobutylene                          | 1.3             | 1.1  | 0.7  | 0.3  | 0.3  |  |
| BTX                                  | 5.5             | 16.6 | 30.1 | 39.7 | 40.9 |  |
| $C_{5+}$                             | 30.1            | 35.9 | 40.1 | 45.5 | 44.8 |  |
| Percentage of BTX in C <sub>5+</sub> | 18              | 46   | 75   | 87   | 91   |  |

(Table 2). At 500 °C, BTX accounts for 91% in the  $C_{5+}$  liquid hydrocarbons and the maximum BTX yield is achieved at 450–500 °C (Table 2). The light olefins ( $C_2$ – $C_4$ ) show a minimum (34%) at 350 °C and light paraffins ( $C_1$ – $C_4$ ) reach a maximum (30%) at this temperature. Among  $C_1$ – $C_4$  hydrocarbons, ethylene is the dominant product in the 300–500 °C range and its lowest yield is at 350 °C (Table 2). The propene yield reaches a maximum at 400 °C but  $C_4$  olefins decrease

with increase in temperature. Both methane and ethane increase gradually with increase in temperature. The maximum yield of propane and other  $C_4$  paraffins reaches a maximum at 350 °C.

3.2.2 Impact of space velocity. The optimization of space velocity is carried out at 450 °C since this is the temperature of the optimum BTX yield (Table 2) at 1.6 h<sup>-1</sup>. A comparison of the product stream for H-ZSM-5 and Ga-ZSM-5 in the WHSV range of 0.4–3.2 h<sup>-1</sup> is presented in Table 3. The decrease in WHSV leads to an increase in BTX yields for both H-ZSM-5 and Ga-ZSM-5. The highest BTX yield is obtained at 0.4 h<sup>-1</sup> for both catalysts and the addition of Ga significantly increases the BTX yield from 26.0% to 55.3%. Meanwhile, the yield of  $C_3$  and  $C_4$  olefins (propene, 2-butene and isobutylene) from Ga-ZSM-5 is significantly less than that from H-ZSM-5 (e.g., 3.2% from Ga-ZSM-5 and 17.8% over H-ZSM-5 at 0.4 h<sup>-1</sup>). These results suggest that Ga promotes the oligomerization & dehydrocyclization of olefins to form BTX, which is consistent with the findings of Choudhary et al. <sup>27</sup>

Furthermore, the reduced formation of propane and butanes over Ga-ZSM-5 can be attributed to the Ga role of suppressing the hydrogen transfer reaction and enhancing hydrogen desorption. This is further supported by the significant difference in  $\rm H_2$  formation over H-ZSM-5 (trace) and Ga-ZSM-5 (~21–25 mol%) in the 0.4–3.2 h<sup>-1</sup> WHSV range. This observation is consistent with the conclusion of Iglesia *et al.* that the hydrogen transfer to hydrocarbon fragments to form light paraffins occurs on H-ZSM-5 while Ga-ZSM-5 proceeds predominantly through the recombinative desorption of H-atoms to form  $\rm H_2$ . <sup>26</sup> Direct conversion of butanes on Ga-ZSM-5 under our reaction conditions is also likely. <sup>28</sup>

The aromatic product distribution also varies with WHSV (Fig. 3). Benzene, toluene, and  $C_{9+}$  decrease with increase in WHSV while ethylbenzene and xylenes increase slightly. This is very likely due to more transalkylations and cracking reactions at lower WHSV.

3.2.3 The effect of Ga loading. Since both methane and ethane are very stable, we do not anticipate their participation in the subsequent reactions under our reaction conditions (300–500 °C and 1 atm).<sup>29</sup> When temperature increases from 300 to 500 °C, methane & ethane yields increase for all the catalysts (Fig. 4a), which is likely due to an enhanced thermal

Table 3 Product distributions for H-ZSM-5 and 6.2% Ga-ZSM-5 at 450 °C

|          | WHSV, h <sup>-1</sup> | $CH_4 \& C_2H_6$ | $C_2H_4$ | $C_3^{=} \& C_4^{=a}$ | $C_3H_8$ | Butanes | $\mathrm{C}_{5^+}$ | BTX  | $H_2^b \text{ (mol\%)}$ |
|----------|-----------------------|------------------|----------|-----------------------|----------|---------|--------------------|------|-------------------------|
| H-ZSM-5  | 0.4                   | 5.1              | 17.5     | 17.8                  | 21.3     | 10.4    | 27.8               | 26.0 | Trace                   |
|          | 0.8                   | 3.8              | 17.4     | 20.1                  | 19.8     | 12.5    | 26.4               | 23.6 | Trace                   |
|          | 1.6                   | 2.8              | 18.2     | 22.8                  | 17.0     | 13.8    | 25.5               | 20.5 | Trace                   |
|          | 3.2                   | 2.1              | 25.7     | 27.6                  | 13.3     | 13.7    | 22.1               | 16.8 | Trace                   |
| Ga-ZSM-5 | 0.4                   | 11.7             | 13.1     | 3.4                   | 7.8      | 1.3     | 62.9               | 55.3 | 25                      |
|          | 0.8                   | 9.5              | 18.5     | 5.0                   | 7.6      | 2.7     | 56.6               | 52.2 | 25                      |
|          | 1.6                   | 7.5              | 27.6     | 7.0                   | 6.2      | 3.8     | 47.9               | 42.9 | 23                      |
|          | 3.2                   | 4.6              | 38.9     | 9.1                   | 4.8      | 5.0     | 37.6               | 29.5 | 21                      |

<sup>&</sup>lt;sup>a</sup>C<sub>3</sub> & C<sub>4</sub> refer to propene, isobutylene and 2-butene. <sup>b</sup>H<sub>2</sub> (mol%) based on ethanol are calculated from the C and H mole balance.

Green Chemistry Paper

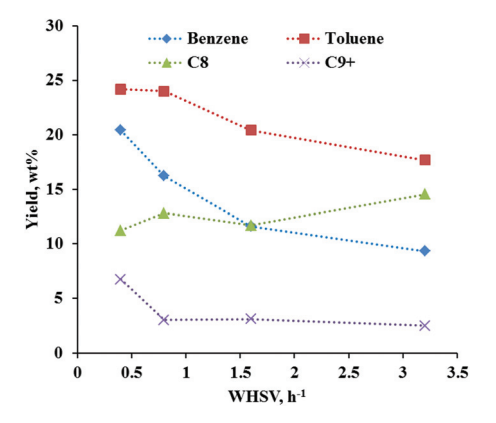


Fig. 3 Aromatic distributions vs. space velocity over 6.2% Ga-ZSM-5 at 450  $^{\circ}\mathrm{C}.$ 

cracking reaction at a higher temperature. Interestingly, Ga-ZSM-5 catalysts produce more methane and ethane than H-ZSM-5, and their yields increase as Ga loadings increase. This is probably due to the enhanced cracking reactions after the introduction of Ga sites as suggested by Rane  $et\ al.$ 

Unlike methane and ethane, the impacts of the Ga loading and reaction temperature on propane yields are different. For H-ZSM-5, the propane yield increases to  $\sim$ 21% at 400  $^{\circ}$ C,

remains at this level until 450 °C, and then decreases to  $\sim$ 15% at 500 °C (Fig. 4b). The Ga incorporation at a low loading ( $\sim$ 0.5%) has a dramatic effect on the propane yield which does not increase beyond  $\sim$ 11%. The increase in the Ga loading to 1.7% results in a further decreased propane yield ( $\sim$ 8%) at 350 °C. The further increase in the Ga loading does not lead to additional reduction in the propane yield. Butane follows a similar trend to propane but the maximum yield is obtained at 350 °C for both H-ZSM-5 and Ga-ZSM-5 catalysts (Fig. 4c).

While the temperature does not have any impact on hydrogen production for H-ZSM-5, the  $\rm H_2$  formation over Ga-ZSM-5 increases with temperature and Ga loadings (Fig. 5a). A clear correlation between the  $\rm C_3$  &  $\rm C_4$  light paraffins and hydrogen production is shown Fig. 5b, and this helps explain the role of Ga in promoting recombinative hydrogen desorption and suppressing hydrogen transfer reactions for light paraffin formation.

Both  $C_{5+}$  and BTX yields depend on the Ga loading and catalyst temperature. For H-ZSM-5,  $C_{5+}$  slightly increases in the temperature range of 300–350 °C and then decreases to 21% above these temperatures (Fig. 6a). BTX follows a similar trend and reaches a maximum at 400 °C (Fig. 6b). For Ga-ZSM-5, both  $C_{5+}$  and BTX increase with temperature and Ga loading. Above 400 °C, the Ga promotion effect becomes more pronounced as Ga-ZSM-5 catalysts produce much higher  $C_{5+}$  and BTX than H-ZSM-5. This result is consistent with reported

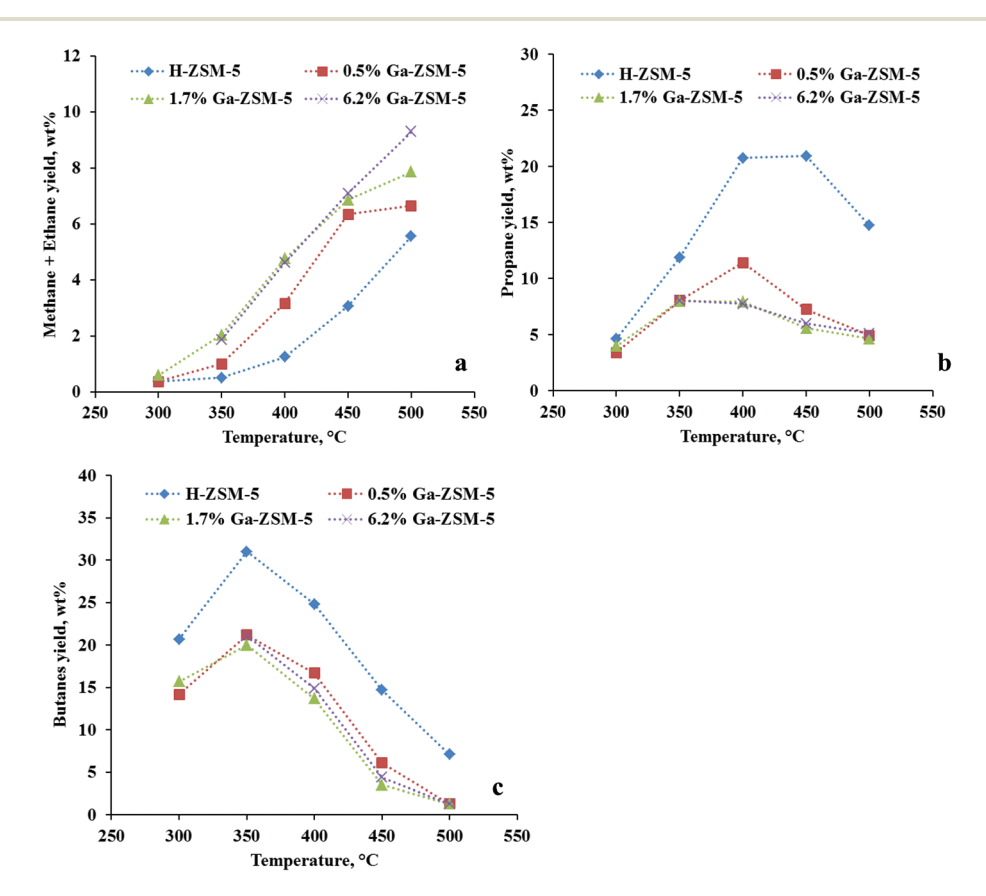


Fig. 4 (a) Methane + ethane, (b) propane and (c) butanes yields for H-ZSM-5 and Ga-ZSM-5 with different Ga loadings at 1.6  $h^{-1}$  from 300 °C to 500 °C.

**Paper** 

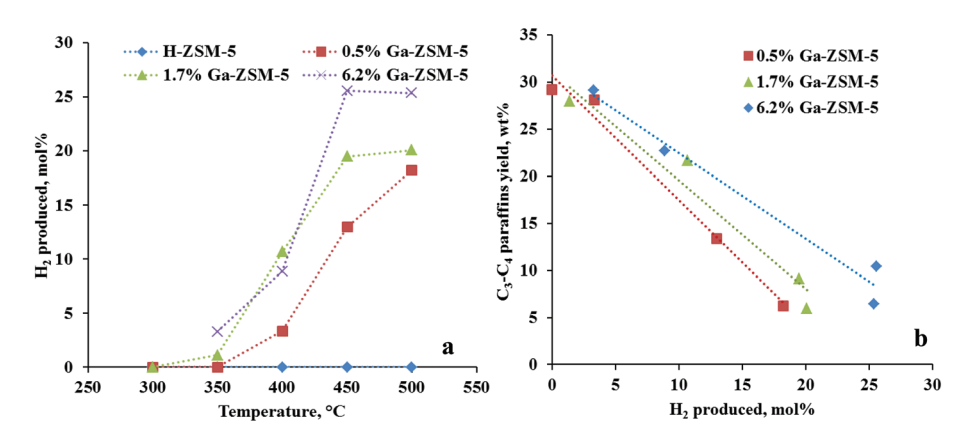


Fig. 5 (a)  $H_2$  production as a function of temperature for H-ZSM-5 and Ga-ZSM-5; (b) correlation between  $C_3 \& C_4$  paraffins and  $H_2$  production on Ga-ZSM-5 with different Ga loadings at 1.6 h<sup>-1</sup>.

observations that Ga has no significant impact on BTX yields at  $\sim$ 350 °C.<sup>20,21</sup> At 500 °C, C<sub>5+</sub> and BTX yields are 50% and 46% respectively over 6.2% Ga-ZSM-5 which are twice as much as that over H-ZSM-5 (21% C<sub>5+</sub> and 18.4% BTX).

#### 3.3 Active Ga species

We tested pure  $\beta$ -Ga<sub>2</sub>O<sub>3</sub> for ethanol conversion and the product stream showed primarily acetaldehyde and acetone with only small amounts of light hydrocarbons, *e.g.*, ethylene (Fig. S1†), and no aromatics. This product stream is very different from that obtained from ethanol conversion over H-ZSM-5. We also performed ethanol conversion over physical mixtures of  $\beta$ -Ga<sub>2</sub>O<sub>3</sub>/H-ZSM-5 with different Ga<sub>2</sub>O<sub>3</sub> loadings (5.9%, 15% and 50% Ga<sub>2</sub>O<sub>3</sub>) and the results showed that the BTX yield and the product distributions are all very similar to that over H-ZSM-5 (Fig. 7, S2 and Table S3†). These results suggest that the physical contact/interface between H-ZSM-5 and extra-zeolitic  $\beta$ -Ga<sub>2</sub>O<sub>3</sub> does not contribute to the promotion effect although the participation of smaller Ga<sub>2</sub>O<sub>3</sub> nanoparticles or other Ga<sub>2</sub>O<sub>3</sub> phases cannot be completely ruled out.

Unlike the transition metal oxides (e.g., Mo, Cr, Fe),<sup>31</sup> Ga(III) is very difficult to reduce under our reaction conditions.

Previous reports, employing XANES,32 show that the Ga species remains unchanged as Ga(III) even under hydrogen reduction at 600 °C and the nearest neighbors of Ga change from OH to H (hydride), which reduces the size of Ga species. The neighboring Brønsted acid sites facilitate the migration of these smaller Ga species into zeolite pores and exchange with the Brønsted acid sites. In our experiments, the physical mixture with 5.9% Ga<sub>2</sub>O<sub>3</sub> loading (4.4% Ga) after hydrogen reduction shows a decrease in Brønsted acid sites from 686  $\mu mol~g^{-1}$  to 613  $\mu mol~g^{-1}$  suggesting that Ga exchanges with the Brønsted acid sites. The BTX yield dramatically increases from ~19% to 49% after hydrogen reduction. The C<sub>5+</sub> yield and distribution also shift to a similar level to 4.4% Ga-ZSM-5 prepared by the ion exchange method (Table S3 and Fig. S3†). These dramatic changes are very likely due to the formation of the exchanged Ga(III) sites during the hydrogen reduction, clearly suggesting that these exchanged Ga(III) cations are involved in the active sites and responsible for the BTX promotion. This physical mixture experiment also suggests an economical and environmentally friendly nonaqueous method for large scale catalyst synthesis without sacrificing catalyst performance.

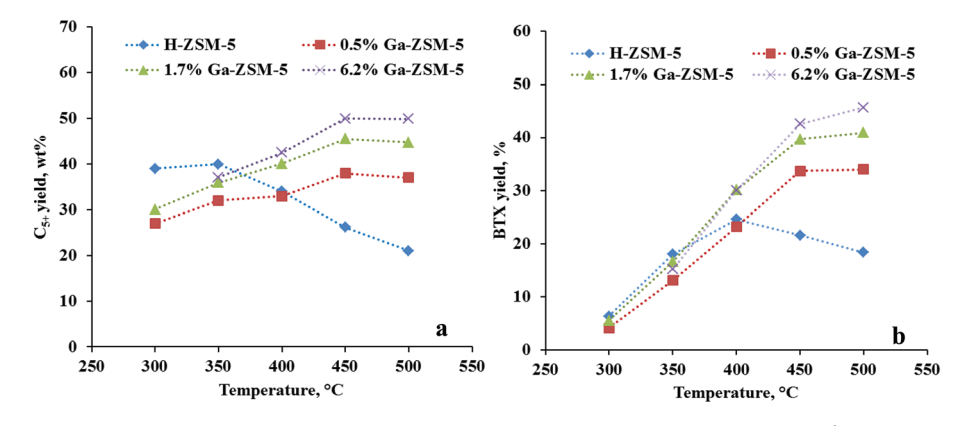


Fig. 6 (a)  $C_{5+}$  and (b) BTX yield vs. temperature for H-ZSM-5 and Ga-ZSM-5 with different Ga loadings at 1.6 h<sup>-1</sup>.

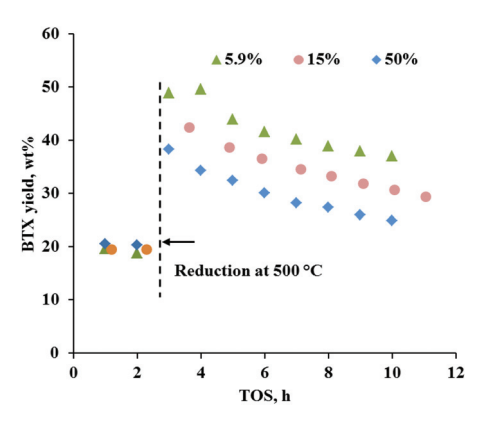


Fig. 7 BTX yield for physical mixtures of  $Ga_2O_3/H$ -ZSM-5 with different  $Ga_2O_3$  loadings before and after hydrogen reduction at 500 °C. Reaction conditions: 450 °C and 1.6  $h^{-1}$ .

Furthermore, we observed a linear correlation between the BTX site time yield and the exchanged Ga sites (Fig. 8). This again strongly supports that the exchanged Ga cation species are involved in the active sites for the BTX promotion effect. Similar active Ga sites have been proposed for propane aromatization by Nowak *et al.* who conclude that the ion-exchanged Ga species are responsible for the enhanced performance of Ga-ZSM-5 during propane aromatization.<sup>25</sup>

The increase in the  $Ga_2O_3$  loading for the physical mixtures to 15% and 50% leads to decreased BTX yields after hydrogen reduction although they remain above those obtained on H-ZSM-5. The liquid hydrocarbon ( $C_{5+}$ ) product distributions from these physical mixtures after hydrogen pretreatment are still similar to ion-exchanged Ga-ZSM-5 (Table S3†). More exchange of Ga is observed for higher  $Ga_2O_3$  loadings as indicated by the larger decrease of the Brønsted acid sites (Table 4).

Since the Brønsted acid sites are also very important during the hydrocarbon transformation, 30,33 a balance between the

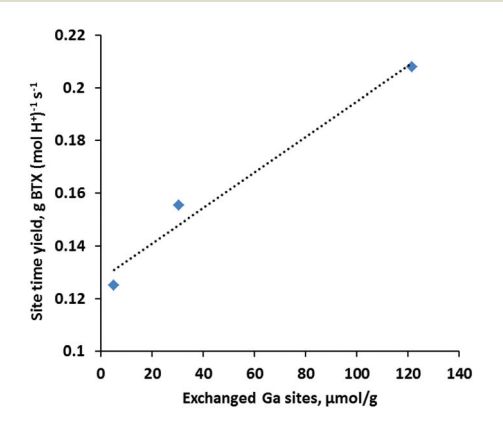


Fig. 8 The relationship between the BTX site time yield and exchanged Ga sites at 450 °C based on ion-exchanged Ga-ZSM-5 catalysts with different Ga loadings. The BTX site time yield is calculated by the BTX production rate (g s $^{-1}$ ) normalized by the moles of the available Brønsted acid sites.

**Table 4** Brønsted acidity for physical mixtures of  $Ga_2O_3$  and H-ZSM-5 with different  $Ga_2O_3$  loadings before and after 500 °C hydrogen reduction

| Sample                                     | Before reduction,<br>μmol g <sup>-1</sup> | After reduction, $\mu$ mol $g^{-1}$ | Changes,<br>% |
|--|---|-------------------------------------|---------------|
| 5.9% Ga <sub>2</sub> O <sub>3</sub> /ZSM-5 | 686                                       | 613                                 | 11            |
| 15% Ga <sub>2</sub> O <sub>3</sub> /ZSM-5  | 621                                       | 414                                 | 33            |
| 50% Ga <sub>2</sub> O <sub>3</sub> /ZSM-5  | 365                                       | 212                                 | 42            |

exchanged Ga sites and the remaining Brønsted acid sites (B) is needed to achieve the optimum BTX formation. As shown in Fig. 9, the optimum exchanged Ga/(exchanged Ga + B) ratio is 0.11 (5.9% Ga<sub>2</sub>O<sub>3</sub>/H-ZSM-5 physical mixture).

#### 3.4 Mechanistic pathways

The conversion of ethanol over M-ZSM-5 (M = H, metals) has been proposed to occur via a dual cycle hydrocarbon pool pathway. While the actual reaction mechanism is more complex, here we mainly examine the possible role of Ga during ethanol conversion (illustrated in the highlighted reaction routes shown in Scheme 1). Ethylene and diethyl ether probably from ethanol dehydration dominate at low temperatures (<300 °C, Fig. S4a†) but can also be one of the products from the aromatic cycle of the hydrocarbon pool in analogy to

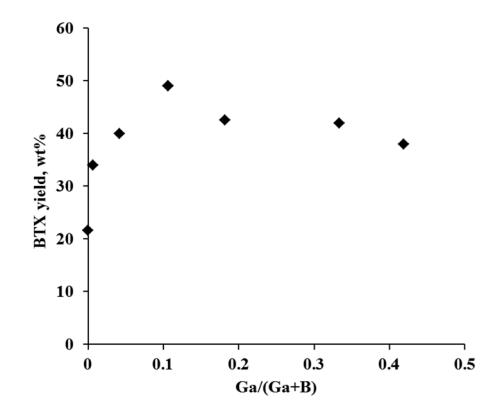
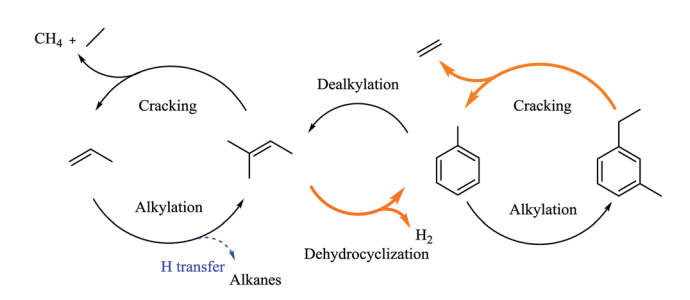


Fig. 9 BTX yield vs. exchanged Ga/(exchanged Ga + B) ratio based on H-ZSM-5, Ga-ZSM-5 and physical mixtures of  $Ga_2O_3/H$ -ZSM-5 at 450 °C and 1.6 h<sup>-1</sup>. B: Remaining Brønsted acid sites.



**Scheme 1** Proposed Ga role for ethanol conversion over Ga-ZSM-5: orange lines (promoted reactions) and blue dashed line (suppressed reaction).

**Paper** 

methanol to hydrocarbon conversion. 35,36 Although the total acid sites of Ga-ZSM-5 are similar to those of H-ZSM-5 (Table 1), ethylene formation is significantly higher than that over H-ZSM-5 (Fig. S4a†). This is probably due to ethylene being one of the products from the aromatic-based cycle which is propagated by Ga addition as evinced by the increased BTX formation.

Another role of Ga is the promotion of oligomerization & dehydrocyclization reactions to convert light olefins (propylene and butenes) to aromatics. As shown in Fig. S4b and S4c,† both propylene and butenes are much lower on Ga-ZSM-5 than on H-ZSM-5, especially above 400 °C, where Ga promotion is more dramatic. Hydrogen production is also largely enhanced due to this promotion effect and the recombinative hydrogen desorption as discussed in the preceding section, which greatly suppresses the light alkane (propane and butanes) formation (Fig. 5).

# Conclusions

This study has shown that Ga-ZSM-5 is able to convert ethanol to BTX in high yields. At 450 °C and 0.4 h<sup>-1</sup>, Ga-ZSM-5 produces 55.3% BTX which is a two-fold increase over H-ZSM-5 (26.0% BTX). The BTX yield increases with increase in temperature (300-500 °C) and Ga loading (0.5% to 6.2%). Enhanced hydrogen production and reduced light paraffin (propane and butane) formation are also observed with the increase of the Ga loading. These results demonstrate that Ga plays an important role in promoting oligomerization & dehydrocyclization and recombinative hydrogen desorption, and suppressing the hydrogen transfer reaction for light alkane formation.

For ion-exchanged Ga-ZSM-5, the majority of Ga is present as extra-zeolitic Ga<sub>2</sub>O<sub>3</sub> particles on the outer surface of the zeolite crystal and only a small fraction of Ga resides in the exchanged positions of H-ZSM-5. The interface between Ga<sub>2</sub>O<sub>3</sub> and H-ZSM-5 is not involved in the active sites for the BTX promotion as demonstrated in our physical mixture experiments. The physical mixtures with reduction experiments show that part of the Ga sites migrate and exchange with the Brønsted acid sites, leading to the increase of BTX formation, which suggests that the exchanged Ga is involved in the active sites. The amount of exchanged Ga cations is found to correlate with the BTX site time yield, strongly supporting the proposed active Ga species. The experiments with physical mixtures of Ga<sub>2</sub>O<sub>3</sub> and H-ZSM-5 also suggest an economical and environmentally friendly non-aqueous method for large scale catalyst synthesis without sacrificing catalyst performance for ethanol conversion application.

# Conflict of interest

The authors declare the following competing financial interest(s): the technology described in this work is licensed to Vertimass

LLC, and two of the authors (Chaitanya K. Narula and Brian H. Davison) are minority owners of Vertimass, LLC.

# Acknowledgements

This research is sponsored by the BioEnergy Technologies Office, Office of Energy Efficiency and Renewable Energy, U.S. Department of Energy, under contract DE-AC05-00OR22725 with UT-Battelle, LLC. GSF and ZW are supported by the U.S. Department of Energy, Office of Science, Office of Basic Energy Sciences, Chemical Sciences, Geosciences, and Biosciences Division. The n-propylamine TPD work was conducted at the Center for Nanophase Materials Sciences, which is a DOE Office of Science User Facility. The assistance of Dr Ercan Cakmak and Dr Harry Meyer for XRD and XPS analysis respectively is greatly acknowledged. We also thank Dr Todd Toops and Dr Andrew Binder for assisting with the NH3-TPD experiments. This manuscript has been authored by UT-Battelle, LLC under Contract No. DE-AC05-00OR22725 with the U.S. Department of Energy. The United States Government retains and the publisher, by accepting the article for publication, acknowledges that the United States Government retains a non-exclusive, paid-up, irrevocable, world-wide license to publish or reproduce the published form of this manuscript, or allow others to do so, for United States Government purposes. The Department of Energy will provide public access to these results of federally sponsored research in accordance with the DOE Public Access Plan (http://energy.gov/downloads/ doe-public-access-plan).

# References

- 1 J. Sun and Y. Wang, ACS Catal., 2014, 4, 1078-1090.
- 2 S. I. Mussatto, G. Dragone, P. M. R. Guimarães, J. P. A. Silva, L. M. Carneiro, I. C. Roberto, A. Vicente, L. Domingues and J. A. Teixeira, Biotechnol. Adv., 2010, 28, 817-830.
- 3 M. Balat and H. Balat, Appl. Energy, 2009, 86, 2273-2282.
- 4 Greenfacts, http://www.greenfacts.org/en/biofuels/figtableboxes/figure-16.htm.
- 5 Environmental Protection Agency, Regulation for Fuels and Fuel Additives: 2012 Renewable Fuel Standards, 40 CFR Part 80, 2012.
- 6 A. P. Kagyrmanova, V. A. Chumachenko, V. N. Korotkikh, V. N. Kashkin and A. S. Noskov, Chem. Eng. J., 2011, **176-177**, 188-194.
- 7 G. Chen, S. Li, F. Jiao and Q. Yuan, Catal. Today, 2007, 125, 111-119.
- 8 A. T. Aguayo, A. G. Gayubo, A. Atutxa, M. Olazar and J. Bilbao, Ind. Eng. Chem. Res., 2002, 41, 4216-4224.
- 9 S. Ogo, A. Onda, Y. Iwasa, K. Hara, A. Fukuoka and K. Yanagisawa, J. Catal., 2012, 296, 24–30.
- 10 S. Ogo, A. Onda and K. Yanagisawa, Appl. Catal., A, 2011, 402, 188-195.

**Green Chemistry** Paper

- 11 T. Tsuchida, J. Kubo, T. Yoshioka, S. Sakuma, T. Takeguchi and W. Ueda, J. Catal., 2008, 259, 183-189.
- 12 M. D. Jones, Chem. Cent. J., 2014, 8, 53.
- 13 E. V. Makshina, W. Janssens, B. F. Sels and P. A. Jacobs, Catal. Today, 2012, 198, 338-344.
- 14 Y. Sekiguchi, S. Akiyama, W. Urakawa, T. R. Koyama, A. Miyaji, K. Motokura and T. Baba, Catal. Commun., 2015, 68, 20-24,
- 15 C. K. Narula, Z. Li, E. M. Casbeer, R. A. Geiger, M. Moses-Debusk, M. Keller, M. V. Buchanan and B. H. Davison, Sci. Rep., 2015, 5, 16039.
- 16 M. B. Frederic Leusch, A short primer on benzene, toluene, ethylbenzene and xylenes (BTEX) in the environment and in hydraulic fracturing fluids, 2010.
- 17 F. Ferreira Madeira, K. Ben Tayeb, L. Pinard, H. Vezin, S. Maury and N. Cadran, Appl. Catal., A, 2012, 443-444, 171-180.
- 18 A. Széchényi, R. Barthos and F. Solymosi, Catal. Lett., 2006, 110, 85-89.
- 19 R. Barthos, A. Széchényi and F. Solymosi, J. Phys. Chem. B, 2006, 110, 21816-21825.
- 20 S. K. Saha and S. Sivasanker, Catal. Lett., 1992, 15, 413-418.
- 21 K. Borght, V. V. Galvita and G. B. Marin, Appl. Catal., A, 2015, 504, 621-630.
- 22 L. G. Price and V. Kanazirev, J. Catal., 1990, 126, 267-278.
- 23 B. Kwak, W. Sachtler and W. Haag, J. Catal., 1994, 149,
- 24 A. Bhan, S. H. Hsu, G. Blau, J. M. Caruthers, V. Venkatasubramanian and W. N. Delgass, J. Catal., 2005, 235, 35-51.

- 25 I. Nowak, J. Quartararo, E. G. Derouane and J. C. Védrine, Appl. Catal., A, 2003, 251, 107-120.
- 26 J. A. Biscardi and E. Iglesia, Catal. Today, 1996, 31, 207-231.
- 27 V. R. Choudhary, D. Panjala and S. Banerjee, Appl. Catal., A, 2002, 231, 243-251.
- 28 Y. Ono and K. Kanae, J. Chem. Soc., Faraday Trans., 1991, 87, 669,
- 29 T. V. Choudhary, E. Aksoylu and D. Wayne Goodman, Catal. Rev., 2003, 45, 151-203.
- 30 N. Rane, M. Kersbulck, R. A. van Santen and E. J. M. Hensen, Microporous Mesoporous Mater., 2008, 110, 279-291.
- 31 J. Gao, Y. Zheng, G. B. Fitzgerald, J. de Joannis, Y. Tang, I. E. Wachs and S. G. Podkolzin, J. Phys. Chem. C, 2014, 118, 4670-4679.
- 32 A. Getsoian, U. Das, J. Camacho-Bunquin, G. Zhang, J. Gallagher, B. Hu, S. Cheah, J. Schaidle, D. Ruddy, J. Hensley, T. Krause, L. Curtiss, J. Miller and A. Hock, Catal. Sci. Technol., 2016, 6, 6339.
- R. Choudhary, P. Devadas, S. Banerjee and 33 V. A. K. Kinage, Microporous Mesoporous Mater., 2001, 47, 253-267.
- 34 R. Johansson, S. L. Hruby, J. Rass-Hansen and C. H. Christensen, Catal. Lett., 2009, 127, 1-6.
- 35 X. Sun, S. Mueller, Y. Liu, H. Shi, G. L. Haller, M. Sanchez-Sanchez, A. C. Van Veen and J. A. Lercher, J. Catal., 2014, 317, 185-197.
- 36 S. Ilias, R. Khare, A. Malek and A. Bhan, J. Catal., 2013, 303, 135-140.